ACS APPLIED MATERIALS & INTERFACES

Research Article

www.acsami.org

Sub-10 nm Feature Size PS-*b*-PDMS Block Copolymer Structures Fabricated by a Microwave-Assisted Solvothermal Process

Dipu Borah,[†,‡,§] Matthew T Shaw,[†,‡,§,⊥] Justin D Holmes,[†,‡,§] and Michael A Morris[†,‡,§,*]

[†]Materials Chemistry Section, Department of Chemistry, University College Cork, College Road, Cork, Ireland

[‡]Centre for Adaptive Nanostructures and Nanodevices (CRANN), Trinity College Dublin, College Green, Dublin 2, Ireland

[§]Tyndall National Institute, Lee Maltings, Prospect Row, Cork, Ireland

[⊥]Intel Ireland Limited, Collinstown Industrial Estate, Leixlip, Co. Kildare, Ireland

ABSTRACT: Block copolymer (BCP) microphase separation at surfaces might enable the generation of substrate features in a scalable, manufacturable, bottom-up fashion provided that pattern structure, orientation, alignment can be strictly controlled. A further requirement is that self-assembly takes place within periods of the order of minutes so that continuous manufacturing processes do not require lengthy pretreatments and sample storage leading to contamination and large facility costs. We report here microwave-assisted solvothermal (in toluene environments) self-assembly and directed self-assembly of a very low molecular weight cylinder-forming polystyrene-*block*-polydimethylsiloxane (PS-*b*-PDMS) BCP on planar and patterned silicon nitride (Si_3N_4) substrates. Good pattern ordering was achieved in the order of minutes. Factors affecting BCP self-assembly, notably anneal time and temperature were studied and seen to have significant effects. Graphoepitaxy to direct self-assembly in the BCP yielded promising results producing BCP patterns with long-range translational alignment commensurate with the pitch period of the topographic patterns. This rapid BCP ordering method is consistent with the standard thermal/solvent anneal processes.

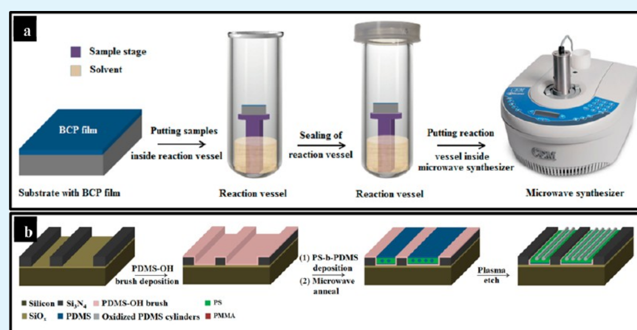

KEYWORDS: *polymer brush, block copolymer, silicon nitride substrate, solvothermal process, microwave anneal, self-assembly, graphoepitaxy, plasma etching, nanoscale patterns*

■ INTRODUCTION

The production of nanostructured surfaces of ever decreasing feature size for use in computing devices is centered around manufacturing methods that allow fabrication at relatively low-cost, high-throughput and, importantly, in short processing periods (the particular focus of this work).[1,2] However, conventional UV-lithography based "top-down" processes are facing significant technical and cost challenges.[3−5] Block copolymer (BCP) lithography is a "bottom-up" process relying on microphase separation in thin films and offers promise for the fabrication of nanopatterns of sub-10 nm scale features and has the potential to integrate into existing manufacturing processes.[6] Excellent control over pattern dimension and structure can be achieved in BCP systems through variation of the molecular weight (N), relative volume fraction (ϕ) and the segmental interaction parameter (χ) and a number of different morphological structures viz., lamellar, cylindrical, spherical, gyroidal, etc.,[7,8] can all be formed.

Despite the apparent advantages of the BCP based methods, a number of important challenges remain and have been the subject of much research. These include: (i) achieving patterns with long-range translational alignment (to a surface feature) and orientation (to the surface plane) control[9−14] and (ii) generating patterns of very low defectivity.[15−18] A less addressed challenge is the need to process pattern development in relatively short times commensurate with high wafer throughput used in the semiconductor industry.[19,20] Microphase separation in BCP thin films is normally achieved using thermal or solvent annealing that can be time-consuming (from several hours to days). Microwave assisted annealing is an emerging technique that affords an opportunity to develop well-ordered patterns in very short process times but as yet the method is less well-researched and is largely unproven in terms of its capability to generate pattern transferred features.

Polystyrene-*block*-polydimethylsiloxane (PS-*b*-PDMS) is an attractive system to study.[21−29] Its Flory−Huggins parameter ($\chi = 68/T - 0.037$, where, T = temperature)[30] is relatively high allowing sub-10 nm feature size scaling.[9,31−33] A further attractive feature of this system is the potential to develop silica based hard-mask structures used for pattern transfer by selective etch methods.[21,28] Following the seminal work of Buriak et al.,[34,35] we report here the nonconventional microwave assisted solvothermal BCP self-assembly on planar and patterned Si_3N_4 substrate process

Received: November 25, 2012
Accepted: February 19, 2013
Published: February 19, 2013

 © 2013 American Chemical Society

to achieve ordering at a faster processing time while demonstrating fabrication capability at small feature sizes. Factors influencing BCP self-assembly such as anneal time and temperature, were investigated. The microwave anneal process was combined with graphoepitaxy to direct self-assembly on patterned Si_3N_4 substrate with variable Si_3N_4 line-widths and pitch period of the trenches to control placement and long-range translational domain alignment.

Table 1. Characteristics of Polymers Used for Present Study

M_n/g mol^{-1}	polymer	polydispersity index, M_w/M_n	PS mole fraction, f_{PS}
5000	PDMS−OH	1.07	
16 000	PS-*b*-PDMS	1.08	0.67

EXPERIMENTAL SECTION

Materials. PS-*b*-PDMS of cylindrical morphology and hydroxyl-terminated PDMS homopolymer brush used in the present investigation were purchased from Polymer Source, Inc., Canada and the detailed characteristics are summarized in Table 1. The substrates used were a low pressure chemical vapor deposition (LPCVD) deposited silicon nitride (Si_3N_4) coated substrate (resistivity, $\rho = 1 \times 10^{14}$ to 1×10^{16} Ω cm) on *p*-type silicon ⟨100⟩ with a surface SiO_2 layer ~7 nm thick. The topographically patterned Si_3N_4 substrates with pitches in the range of 75−500 nm, variable mesa widths of 30−700 nm, and depth of 60 nm were fabricated via 193 nm UV-lithography and processed by means of conventional mask and etch techniques. Sulfuric acid, hydrogen peroxide, ethanol, acetone, iso-propanol (IPA), and toluene were purchased from Sigma-Aldrich and used as received. Deionized (DI) water was used wherever necessary.

Scheme 1. (a) Schematic Showing the Process of Microwave Annealing of BCP Films in the Presence of Solvent in a Microwave Synthesizer to Achieve BCP Ordering; (b) Schematic Representation of the Process Flow Showing BCP Self-Assembly on Si_3N_4 Substrate Precoated with PDMS−OH Brush and Subsequent Plasma Etching (see text for details)

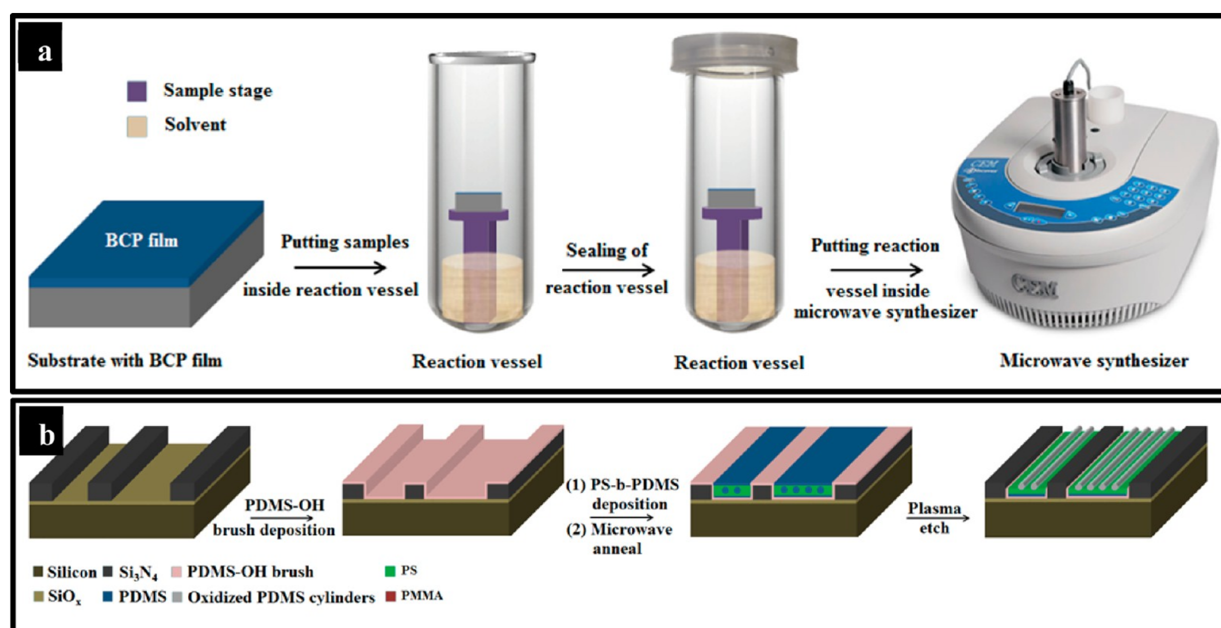

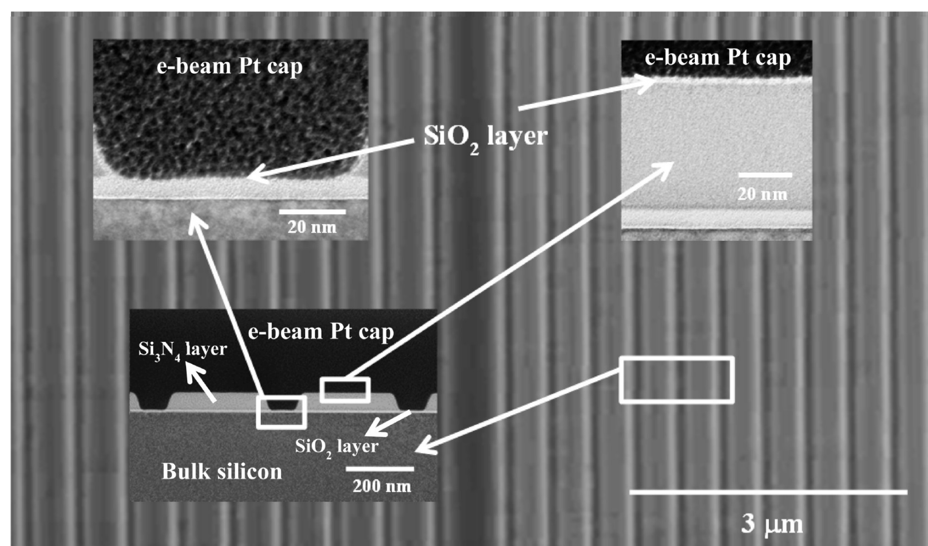

Figure 1. Top-down SEM image of a section of a topographically patterned Si_3N_4 substrate. Insets shows high-resolution cross-section TEM images and demonstrate the composition and depth profile of the channels.

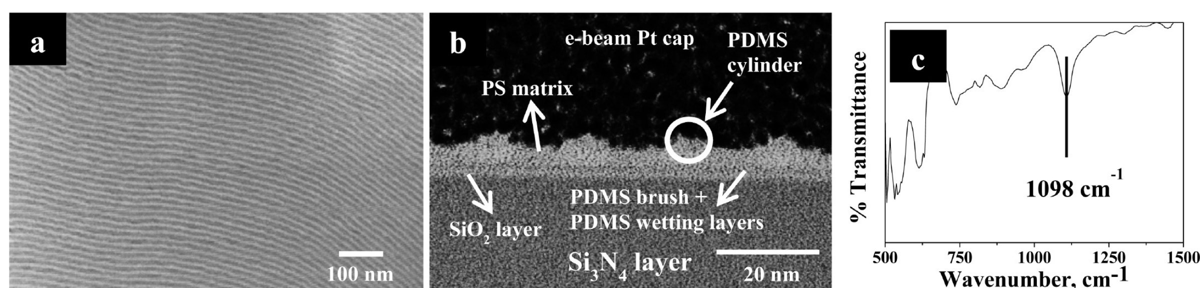

Figure 2. (a) Top-down SEM image of the PS-*b*-PDMS structure at a planar Si_3N_4 substrate following microwave treatment at 323 K for 30 s in toluene (light gray lines are oxidized PDMS and darker lines are voids created following partial PS removal). (b) High-resolution cross-section TEM image of the oxidized PDMS cylinders structure in a. (c) FTIR spectrum of the oxidized PDMS cylinders.

Table 2. Measured Water Contact Angle and Film Thickness (ellipsometery) of Various Films at Planar Substrates, and BCP Domain Size (pitch) as Measured by SEM

material	deposition condition	contact angle (deg)	thickness (nm)	pitch from SEM/nm
Si_3N_4/Si substrate	as received	46.5 ± 1.5		
Si_3N_4/Si substrate	piranha cleaned	32.4 ± 1.5		
PDMS−OH + Si_3N_4/Si substrate	annealed/cleaned	109.5 ± 1.5	4.1 ± 2	
BCP + PDMS−OH + Si_3N_4 substrate	as-cast BCP film (1.0 wt %)		21.5 ± 2	18

Polymer Brush Precoating and BCP Film Preparation. Diced substrates of 0.5 cm^2 were degreased by ultrasonication in acetone and IPA solutions for 5 min each, dried in flowing N_2 gas and baked for 2 min at 393 K in an ambient atmosphere to remove any residual IPA. This was followed by cleaning in a piranha solution (1:3 v/v 30% H_2O_2:H_2SO_4) at 363 K for 60 min, rinsed with DI water, acetone, ethanol and dried under N_2 flow. A hydroxyl-terminated polymer brush solution (1.0 wt % in toluene) was spin-coated (P6700 Series Spin-coater, Specialty Coating Systems, Inc., USA) onto substrates at 3000 rpm for 30 s. Samples were annealed in a vacuum oven (Townson & Mercer EV018) at 443 K under vacuum (−100 kPa). This procedure provides chemically anchored brushes by condensation reactions between −OH groups at the substrate surface and on the brush. Unbound polymers were removed by ultrasonication (Cole-Palmer 8891 sonicator) and rinsing in toluene and then dried for 30 min at 333 K in an ambient atmosphere to remove any residual toluene. A 1.0 wt % toluene solution of PS-*b*-PDMS was spin-coated onto the brush anchored surfaces at 3200 rpm for 30 s and immediately used for microwave irradiation.

Microwave Anneal of BCP Films. Microwave annealing experiments were performed in a microwave synthesizer, CEM Discover LabMate (CEM Microwave Technology Ltd., UK) with the IntelliVent Pressure Control System and CEM's Synergy software. The system focuses microwaves into a sample cavity. The system was computer controlled using CEM's Synergy software so that power, temperature, time and pressure could be precisely controlled. The BCP coated substrates were placed inside the reaction chamber and irradiated with microwave energy. The target temperature was achieved through microwave feedback control where microwave power is used to control temperature. Stable temperatures were reached within 20−100 s depending upon the target temperature. The anneal time (30−180 s) started once the target temperature was achieved. Note that the reaction vessel takes about 30−100 s to cool to ambient conditions after heating. During this period, some organization and assembly of the BCP film is expected. Dewetting of the BCP film was not observed in any of the experiments.

Plasma Etching of BCP Films. PS-*b*-PDMS BCP films show little indication of microphase separated structure in AFM or SEM because

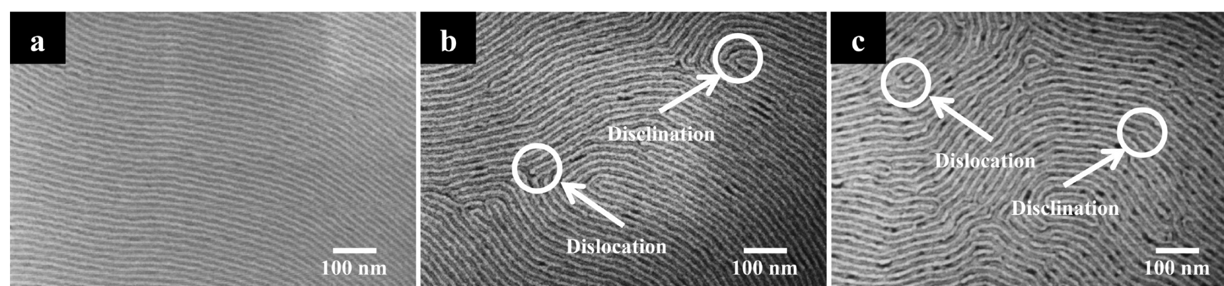

Figure 3. Top-down SEM images of the PS-*b*-PDMS pattern formed via microwave annealing at 323 K for (a) 30, (b) 60, and (c) 180 s in the presence of toluene.

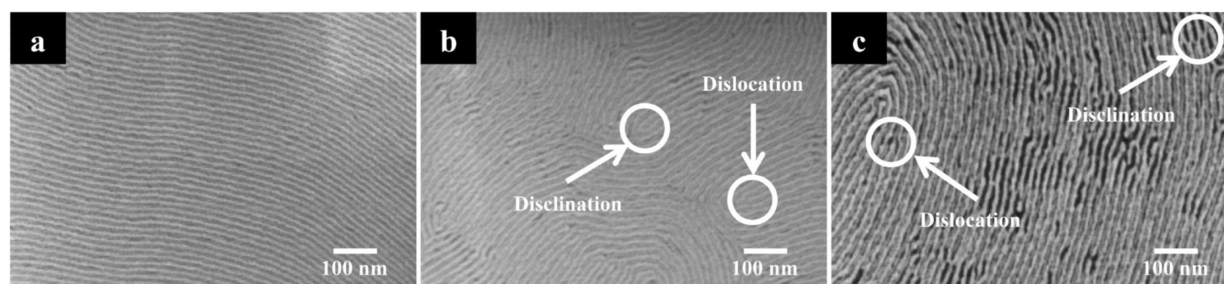

Figure 4. Top-down SEM images of the PS-*b*-PDMS pattern following microwave annealing for 30 s at (a) 323, (b) 373, and (c) 423 K in the presence of toluene.

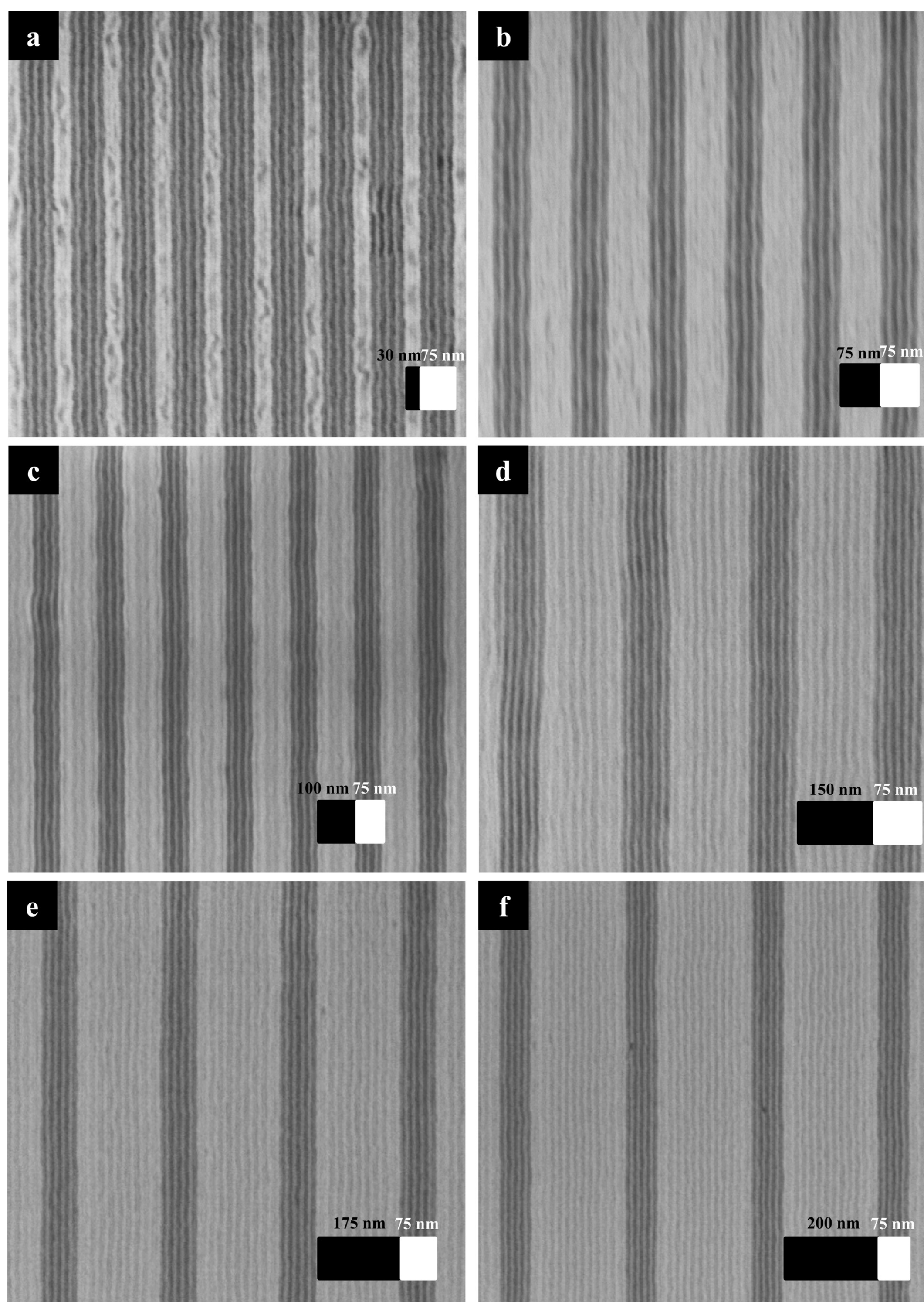

Figure 5. Top-down SEM images of the PS-*b*-PDMS pattern (as revealed by sequential CF_4 and O_2 etches) formed on PDMS−OH brush modified patterned Si_3N_4 substrates. Data shown are varying channel widths as follows: (a) 30, (b) 75, (c) 100, (d) 150, (e) 175, and (f) 200 nm. In all cases, the channel pitch is 75 nm. Darker regions are the channels, lighter regions the mesas.

of the presence of a surface wetting layer of PDMS which must be removed to reveal the BCP arrangement.[21,28] Films were first treated with a CF_4 (15 sccm) plasma for 5 s with an inductively coupled plasma (ICP) and reactive ion etching (RIE) powers of 400 and 30 W, respectively, at 2.0 Pa with a helium backside cooling pressure of 1333.2 Pa to remove any surface PDMS layer. This was followed by an O_2 (30 sccm) plasma for 10 s with an ICP and RIE powers of 1200 and 30 W, respectively, at 2.0 Pa with helium backside cooling pressure of 666.6 Pa. These steps follow similar methodology developed by Ross et al.[28] The process removes the PS component and forms an oxidized form of PDMS on the substrate.

Characterization of Materials. Advancing contact angles (θ_a) of deionized water on the substrates was measured using a Data Physics Contact Angle (model: OCA15) goniometer. Contact angles were measured on the opposite edges of at least five drops and averaged. The values were reproducible to within 1.5°. BCP thin film thickness was

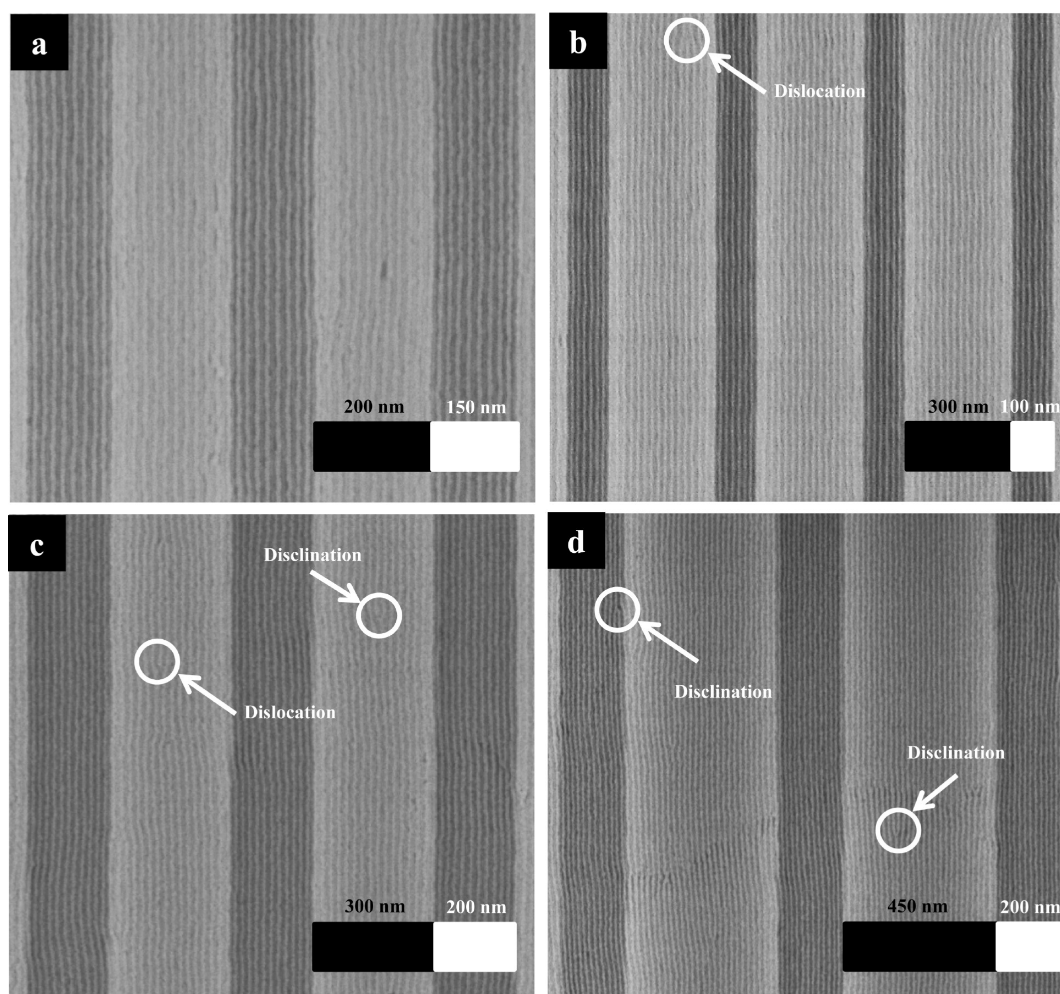

Figure 6. Top-down SEM images of the PS-*b*-PDMS pattern (as Figure 5). Data shown are with Si_3N_4 channel widths and pitches of (a) 200 and 150 nm, (b) 300 and 100 nm, (c) 300 and 200 nm, and (d) 450 and 200 nm.

determined by a spectroscopic ellipsometry (Plasmos SD2000 Ellipsometer) at a fixed angle of incidence of 70°. Quoted film thicknesses were an average of five readings collected from different locations on the sample surface. A two layer model (Si_3N_4 + polymer brush) for polymer brush and a three layer model (Si_3N_4 + polymer brush + BCP) for total BCP film was used to simulate experimental data. A Varian IR 610 infrared spectrometer was used to record the FTIR spectra in the transmittance mode. The measurements were performed in the spectral range of 4000−500 cm^{-1}, with a resolution of 4 cm^{-1} and data averaged over 32 scans. Scanning electron microscope (SEM) images were obtained by a high-resolution (<1 nm) Field Emission Zeiss Ultra Plus-SEM with a Gemini column operating at an accelerating voltage of 5 kV. An FEI Strata 235-Focused Ion Beam (FIB) tool was used to generate FIB lamellae cross sections. E-beam produced platinum was deposited at the substrate followed by the ion-beam deposited platinum. Milling and polishing of the samples were carried out at the lower aperture size and the specimen was imaged under the higher resolution Zeiss Ultra Plus-SEM. The transmission electron microscope (TEM) lamella specimen were prepared by the Zeiss Auriga-FIB with cobra ion column having a unique 2.5 nm resolution and were analyzed by FEI Titan-TEM operating at an accelerating voltage of 130 kV.

■ RESULTS AND DISCUSSION

The microwave assisted BCP process is illustrated in Scheme 1a. The BCP coated substrate was placed in a reaction tube partially filled with solvent, sealed and then irradiated with microwave energy. The BCP self-assembly process steps are shown in Scheme 1b and are:- hydroxyl-terminated polymer brush grafting, microphase separation and plasma treatment to remove the PDMS wetting layer as detailed above.[21,28] Figure 1 shows a top-down SEM image of a section of the patterned substrate along with corresponding TEM cross sections. The inset cross-section TEM images clearly shows three distinct layers in the order Si_3N_4−SiO_2-bulk silicon from top to bottom. A channel depth of ~60 nm can be seen in the image. The high-resolution cross-section images of the channel base and top of the mesa shows the presence of a very thin (~1.5 nm) SiO_2 layer. This oxide layer might have formed at the time of LPCVD deposition and etch pattern development.

■ MICROWAVE-ASSISTED SELF-ASSEMBLY ON PLANAR SUBSTRATES

Microphase separation in cylindrical PS-*b*-PDMS at silicon substrates necessitates use of a PDMS−OH brush to control surface wetting and pattern orientation. The brush results in pattern formation with a wetting PDMS layer at the gas-surface and substrate-BCP interface because of the low surface energy of PDMS and favorable PDMS−PDMS interactions at the brush-BCP interface.[21,28] The formation of this sandwich structure strongly promotes the formation of a BCP pattern where the PDMS cylinders are orientated parallel to the surface plane since any vertical orientation will lead to significant increases in surface energy. Figure 2a shows

dx.doi.org/10.1021/am302830w | ACS Appl. Mater. Interfaces 2013, 5, 2004−2012

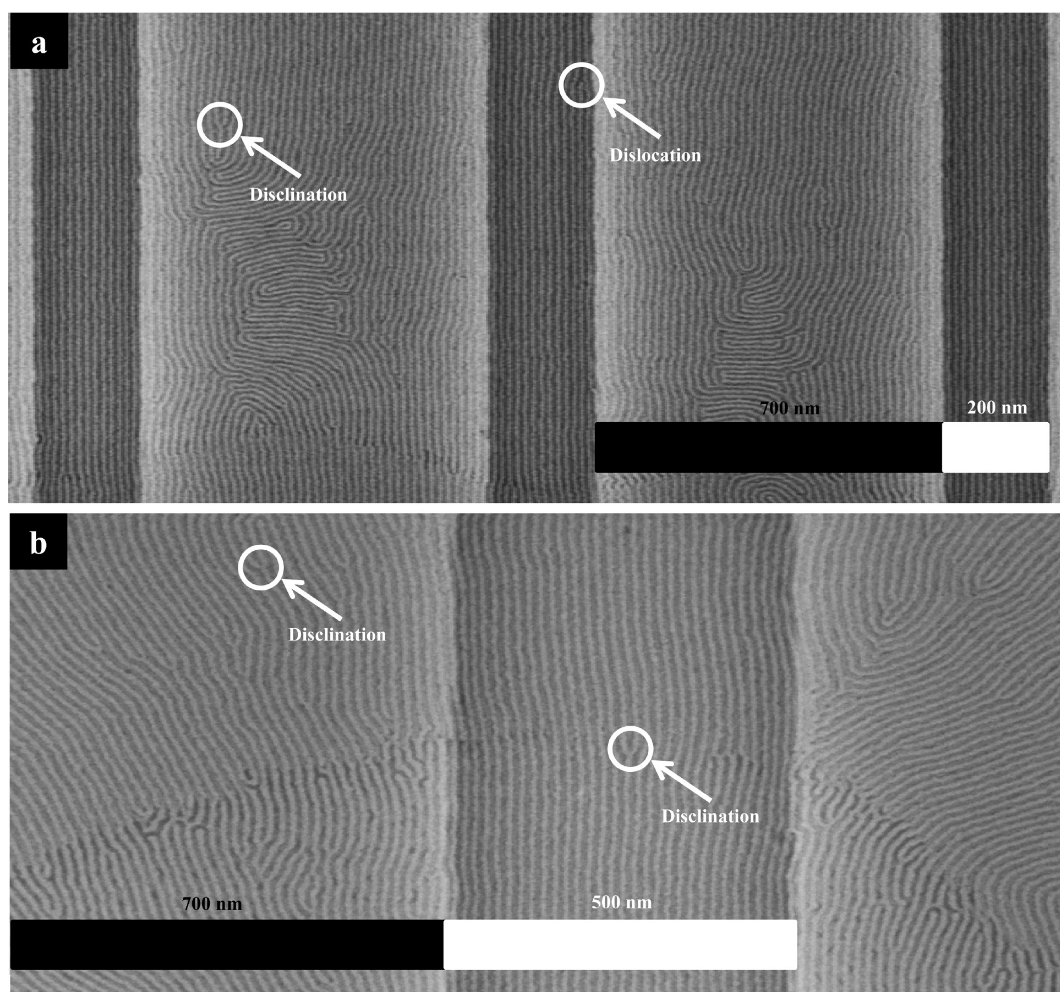

Figure 7. Top-down SEM images of the PS-*b*-PDMS pattern formed on PDMS−OH brush modified patterned Si_3N_4 substrate Data shown are with Si_3N_4 channel widths of 700 nm at pitches of (a) 200 and (b) 500 nm.

oxidized PDMS cylinders (as revealed by the etch methodology) formed from the BCP PS-*b*-PDMS film on a planar Si_3N_4 substrate following microwave processing (323 K for 30 s). The high resolution cross-section TEM image in Figure 2b shows a single monolayer of PDMS cylinders and demonstrates the efficacy of the etch chemistry to reveal the cylindrical patterns. The PDMS cylinders appear to reside in a PS matrix that is partially etched and are ∼8 nm in diameter. A wetting PDMS layer at the substrate surface can also be clearly seen and this is thicker (∼6 nm) (Figure 2b) than the thickness of the PDMS−OH brush layer (∼4 nm) (Table 2) and confirms sufficient PDMS−OH (brush)−PDMS (BCP) interactions. It is clear from the data in Figure 2a, b that well-ordered phase separation is observed. Note that no ordered self-assembly is seen in similar films exposed to the same solvent at the same temperature in the absence of microwave irradiation. This suggests that the microwave annealing method promotes sufficient molecular motion for the BCP to reach its local thermodynamic minimum. The mean PDMS cylinder spacing (cylinder center-to-center), L_0, and line width, $\langle d \rangle$, were found to be 18.0 and 8.0 nm, respectively. It can also be seen from the image that the oxidized PDMS domains have become rounded during the etch process indicating that it is partially isotropic. The oxidation of the PDMS cylinders during this etch step is confirmed by FTIR with the detection of a Si−O−Si signal at 1098 cm^{-1}[36] as displayed in Figure 2c. Dewetting is a major issue with high χ BCP systems such as PS-*b*-PDMS leading to multilayer pattern formation in some locations on the substrate upon solvent annealing.[37] Note that the 1.0 wt % BCP in toluene solution used in film casting provided a continuous film (film thickness ∼21 nm (Table 2), i.e., close to the 18 nm periodicity of PDMS cylinders) and dewetting was not observed after microwave irradiation. This is a significant advantage for application of these films (particularly for subsequent pattern transfer to underlying silicon substrate). The good wetting of the substrate might be related to the efficient heating of the sample and short treatment periods that limit solvent condensation.[37] It should be emphasized that the regularity and structural order of the patterns indicate that the surface interactions between the BCP and the brush coated surface are significantly robust to survive the microwave processing and in particular thermal and mechanical strains that must exist at the interfaces.

Microwave-Assisted Self-Assembly. *Effect of Anneal Time.* The effect of microwave anneal time of the microphase separation of PS-*b*-PDMS is shown in Figure 3. Anneal times were varied from 30 to 180 s at a constant temperature of 323 K. It can be seen that the patterns became more disordered and with increased densities of both dislocation and disclination defect sites as the anneal time increases. This disorder obviously represents kinetic effects. Initially the film is nonmicrophase separated and subsequently orders into regular patterns. Finally,

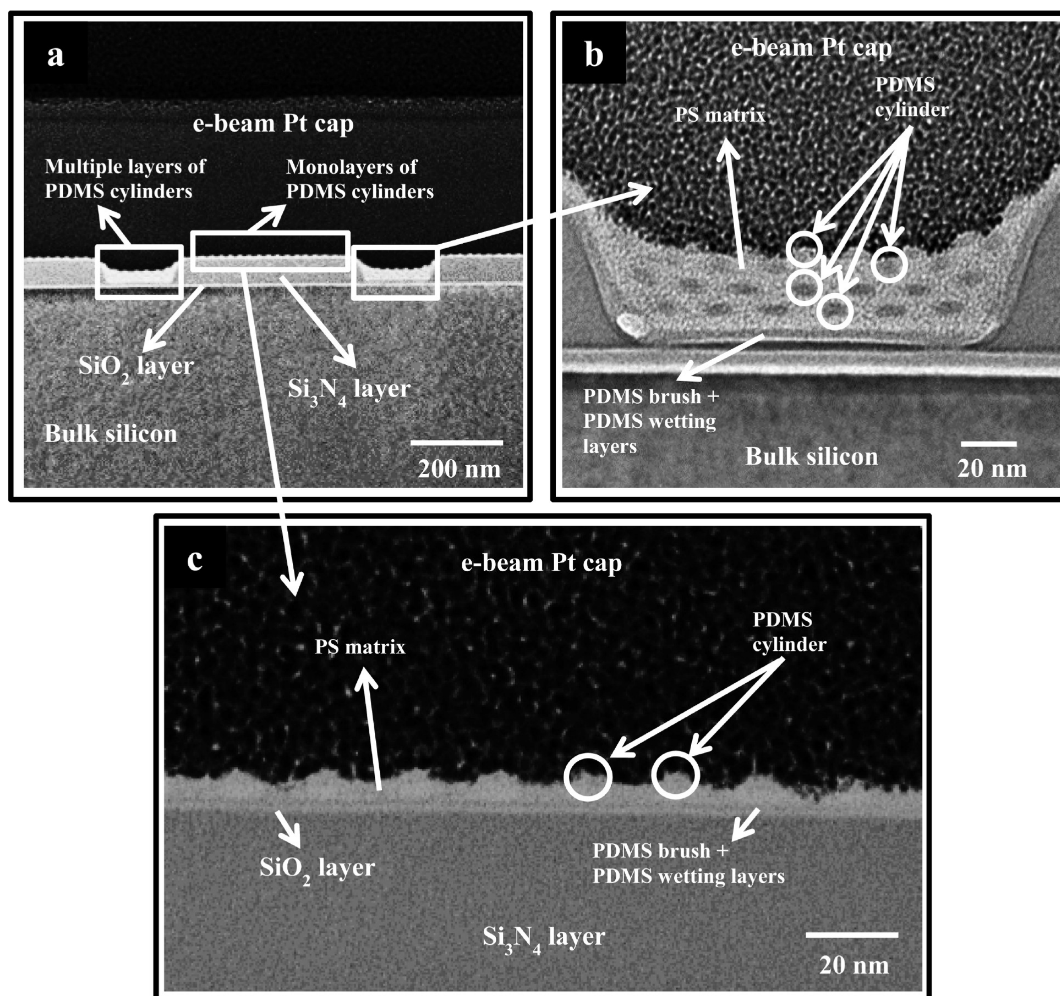

Figure 8. High-resolution cross-section TEM images of the PS-*b*-PDMS pattern (as revealed by sequential CF_4 and O_2 etches) formed on PDMS−OH brush-modified patterned Si_3N_4 substrate and microwave annealed at 323 K for 30 s in the presence of toluene.

the film moves through the order−disorder phase and becomes less well-ordered.[38,39] The kinetic limitations may represent a temperature lag between the substrate and the film or possible the kinetics of solvent swelling. For the BCP film L_0 and ⟨d⟩, were very similar to the values noted above and within experimental error (±1), at 18.1 and 8.0 nm, respectively.

Microwave-Assisted Self-assembly. *Effect of Anneal Temperature.* Clearly, temperature may have a profound effect on the BCP self-assembly into regular nanopatterns. Figure 4 shows the temperature evolution of PS-*b*-PDMS BCP ordering in the temperature range of 323−423 K at a chosen time of 30 s. This time period was judged to be optimal based on the data provided above. Figure 4 shows that a temperature effect is observed.

In Figure 4 it is evident that the correlation length of the in-plane PDMS cylinders decreases and the number of defects increase with the temperature used. However, the changes are not as dramatic as might be expected. These data do suggest that the pattern evolution with time seen above are unlikely to be due to any thermal effects (time lag) and are more likely to be due to solvent swelling effects. The thermal effects can also be described by a similar explanation based around solvent swelling as a minor increase in L_0 and $\langle d \rangle$ was observed with the increase of temperature and the values at the highest temperatures were found to be 18.8 and 8.3 nm, respectively. Solvent swelling is expected to increase with temperature.[40−42] This increase in solvent content also decreases the Flory−Huggins interaction parameter,[24,41] and as a result, it might be expected that disorder would increase as is indeed observed.

Microwave-Assisted Directed Self-Assembly. Realizing the full potential of BCP self-assembled structures is only possible if long-range periodic and translational order can be achieved. Graphoepitaxy to direct the self-assembly of PS-*b*-PDMS has been demonstrated as potentially important.[21−29,31−33,43] Further, microwave assisted BCP graphoepitaxy has been shown for cylinder- forming PS-*b*-PMMA and PS-*b*-P4VP BCPs by Buriak et al.[35] Graphoepitaxial alignment of PS-*b*-PDMS under microwave assisted treatment was attempted here in order to properly define the usefulness of the methodology. The topographically patterned Si_3N_4 substrates were precoated with the PDMS−OH polymer brush as described above for planar wafers. The samples were microwave annealed at 323 K for 30 s. Results are shown Figures 5, 6, and 7. It can be seen from the images that the brush induced microphase separation occurs with cylinder alignment to the topographic channel direction. The observation of parallel alignment of the PDMS domains along the trenches is consistent with the thermodynamically most favorable graphoepitaxial alignment to minimize the strain in the microdomain lattice.[31,33]

From Figures 5, 6, and 7, it can be seen that the BCP is not confined to the channels and significant polymer resides at the

mesas (i.e., the exterior surface of the patterns). Generally, alignment extends from the channels onto the mesas and good graphoepitaxial alignment is seen across the entire surface (several ∼5 μm^2 areas were imaged by SEM) with few defects. This can be most readily seen in Figure 5 where the channel width was fixed at 75 nm and the mesa width was varied. In Figure 6 and 7 that reasonable alignment within channels can be seen to channel widths of 500 nm. However, it can be seen in Figure 7 that the BCP pattern became disordered at the mesas when the mesa width was increased to 700 nm. It shows that there is a critical mesa width beyond which alignment disappears. It should also be noted that at mesa widths of 300 nm and above there is an increasing density of dislocation and disclination defects. The inherent defectivity of these systems is difficult to determine as many of the defects observed at smaller channel sizes probably arise from "errors" in the sidewall which cause local variations in the channel and mesa width which precipitate defects. However, the results show that the methodology is consistent with production of low defect densities and further that the variation in channel width controls the number of cylinders within a channel.

The alignment of the cylinders within the channels allows high resolution electron microscopy to be performed (because the alignment of the cylinders can be very precisely defined for controlled FIB lamellae production). This facilitated very precise understanding of the PS-*b*-PDMS system and TEM data are presented in Figure 8. The cross-section was taken in an area with PDMS domains residing on top of the mesa as well as channels. It is clear that the film at the mesas is a single layer of cylinders thick as etching reveals a single layer of oxidized PDMS cylinders (Figure 8c). What should also be noted is a bilayer of PDMS and oxidized PDMS at the substrate interface. It is thought that the BCP layer at the mesas is strongly favored as the PDMS brush and the PDMS BCP wetting layer strongly interact preventing capillary forces moving material into the channels.

Within the channel (Figure 8b), a cylinder multilayer of four rows of cylinders is seen and only an upper layer of oxidized cylinders is observed. It is clear that the etch does not significantly modify the layers below the upper layer of cylinders. The PDMS wetting layer at the substrate can be readily observed (thickness about 6 nm). It is noticeable that the cylinders within the film have an elliptical shape rather than the expected circular cross-section. We believe this represents in-plane film stress that results from film contraction that occurs because the solvent swelled film during microwave treatment shrinks as solvent evaporates on removal from the reaction vessel. It can be seen that the BCP film formed a continuous layer from the mesa into the channel suggesting that capillary flow has occurred.

■ CONCLUSIONS

Microwave-assisted solvent annealing is seen to be an effective form of processing to yield well-ordered microphase separated block copolymer patterns. The patterns appear to have similar structure and arrangement to films formed by conventional methods.[9,31−33] The technique does not appear to noticeably worsen surface wetting, domain persistence length or alter structural dimensions when compared to similar compositions of block copolymers. However, the key advantage is the ability to form these well-ordered patterns in periods of less than a minute and hence be consistent with large scale manufacturing. It should be noted that microwave annealing of large silicon substrates (for other applications) has been shown to be highly efficient and heat the surface regularly over the whole substrate.[44,45] Not only is pattern formation affected by the microwave treatment, the methodology is consistent with graphoepitaxy and the structure aligns over large areas when both the channel width and mesa width are below a critical size. However, structural alignment is lost at critical distances from the directing topography, but this is consistent with other processing methods.

Interestingly, the TEM analysis reported shows some important information on the structure of these films in topographically patterned surfaces. The data provide good evidence of the capillary flow of polymer from the mesas into the channels as was suggested by Morris et al.[46] previously. The strong interaction of the brush and the BCP prevents complete removal of the polymer from the mesa. It was also seen that the PDMS cylinders have circular or elliptical cross-sections within the film, and this is the first time clear evidence of this has been presented.

■ AUTHOR INFORMATION

Corresponding Author

*E-mail: m.morris@ucc.ie. Phone: +353 214902180. Fax: +353 214274097.

Notes

The authors declare no competing financial interest.

■ ACKNOWLEDGMENTS

Financial support for this work is provided by the EU FP7 NMP project, LAMAND (Grant 245565) project and the Science Foundation Ireland Grant 09/IN.1/602), and gratefully acknowledged.

■ REFERENCES

(1) Park, S.; Kim, B.; Xu, J.; Hofmann, T.; Ocko, B. M.; Russell, T. P. *Macromolecules* **2009**, *42*, 1278−1284.

(2) *International Technology Roadmap for Semiconductors 2007, Emerging Research Materials* Semiconductor Industry Association: San Jose, CA, 2007.

(3) Harriott, L. *Proc. IEEE* **2001**, *89*, 366−374.

(4) Ito, T.; Okazaki, S. *Nature* **2000**, *406*, 1027−1031.

(5) Broers, A. N. *IBM J. Res. Dev.* **1988**, *32*, 502−513.

(6) Black, C. T. *ACS Nano* **2007**, *1*, 147−150.

(7) Hamley, I. W. *The Physics of Block Copolymers*; Oxford University Press: New York, 1998.

(8) Holden, G.; Legge, N. R.; Schroeder, H. E.; Quirk, R. P. *Thermoplastic Elastomers*; Hanser: New York, 1987.

(9) Park, S. M.; Liang, X.; Harteneck, B. D.; Pick, T. E.; Hiroshiba, N.; Wu, Y.; Helms, B. A.; Olynick, D. L. *ACS Nano* **2011**, *5*, 8523−8531.

(10) Jeong, S. J.; Kim, J. E.; Moon, H. S.; Kim, B. H.; Kim, S. M.; Kim, J. B.; Kim, S. O. *Nano Lett.* **2009**, *9*, 2300−2305.

(11) Park, S. M.; Stoykovich, M. P.; Ruiz, R.; Zhang, Y.; Black, C. T.; Nealey, P. F. *Adv. Mater.* **2007**, *19*, 607−611.

(12) Ruiz, R.; Ruiz, N.; Zhang, Y.; Sandstrom, R. L.; Black, C. T. *Adv. Mater.* **2007**, *19*, 2157−2162.

(13) Xiao, S.; Yang, X. M.; Edwards, E. W.; La, Y. -H.; Nealey, P. F. *Nanotechnology* **2005**, *16*, S324−S329.

(14) Segalman, R. A.; Yokoyama, H.; Kramer, E. J. *Adv. Mater.* **2001**, *13*, 1152−1155.

(15) Rasappa, S.; Borah, D.; Senthamaraikannan, R.; Faulkner, C. M.; Shaw, M. T.; Gleeson, P.; Holmes, J. D.; Morris, M. A. *Thin Solid Films* **2012**, *522*, 318−323.

(16) Farrell, R. A.; Kinahan, N. T.; Hansel, S.; Stuen, K. O.; Petkov, N.; Shaw, M. T.; West, L. E.; Djara, V.; Dunne, R. J.; Varona, O. G.; Gleeson, P. G.; Jung, S. -J.; Kim, H. -Y.; Kolesnik, M. M.; Lutz, T.; Murray, C. P.; Holmes, J. D.; Nealey, P. F.; Duesberg, G. S.; Krstić, V. K.; Morris, M. A. *Nanoscale* **2012**, *4*, 3228−3236.

(17) Borah, D.; Shaw, M. T.; Rasappa, S.; Farrell, R. A.; O'Mahony, C.; Faulkner, C. M.; Bosea, M.; Gleeson, P.; Holmes, J. D.; Morris, M. A. *J. Phys. D: Appl. Phys.* **2011**, *44*, 174012−174023.
(18) Farrell, R. A.; Fitzgerald, T. G.; Borah, D.; Holmes, J. D.; Morris, M. A. *Int. J. Mol. Sci.* **2009**, *10*, 3671−3712.
(19) Bang, J.; Jeong, U.; Ryu, D. Y.; Russell, T. P.; Hawker, C. J. *Adv. Mater.* **2009**, *21*, 4769−4792.
(20) Chai, J.; Wang, D.; Fan, X.; Buriak, J. M. *Nat. Nanotechnol.* **2007**, *2*, 500−506.
(21) Hobbs, R. G.; Farrell, R. A.; Bolger, C. T.; Kelly, R. A.; Morris, M. A.; Petkov, N.; Holmes, J. D. *ACS Appl. Mater. Interfaces* **2012**, *4*, 4637−4642.
(22) Jung, Y. S.; Chang, J. B.; Verploegen, E.; Berggren, K. K.; Ross, C. A. *Nano Lett.* **2010**, *10*, 1000−1005.
(23) Jung, Y. S.; Lee, J. H.; Lee, J. Y.; Ross, C. A. *Nano Lett.* **2010**, *10*, 3722−3726.
(24) Jung, Y. S.; Ross, C. A. *Adv. Mater.* **2009**, *21*, 2540−2545.
(25) Bita, I.; Wang, J. K. W.; Jung, Y. S.; Ross, C. A.; Thomas, E. L.; Berggren, K. K. *Science* **2008**, *321*, 939−943.
(26) Jung, Y. S.; Jung, W.; Ross, C. A. *Nano Lett.* **2008**, *8*, 2975−2981.
(27) Ross, C. A.; Jung, Y. S.; Chuang, V. P.; Llievski, F.; Yang, J. K. W.; Bita, I.; Thomas, E. L.; Smith, H. I.; Berggren, K. K.; Vancso, G. J.; Cheng, J. Y. *J. Vac. Sci. Technol. B* **2008**, *26*, 2489−2494.
(28) Jung, Y. S.; Ross, C. A. *Nano Lett.* **2007**, *7*, 2046−2050.
(29) Brinkmann, M.; Chan, V. Z. H.; Thomas, E. L.; Lee, V. L.; Miller, R. D.; Hadjichristids, N.; Avgeropoulos, A. *Chem. Mater.* **2001**, *13*, 967−972.
(30) Nose, T. *Polymer* **1995**, *36*, 2243−2248.
(31) Chang, J. -B.; Son, J. G.; Hannon, A. F.; Alexander-Katz, A.; Ross, C. A.; Berggren, K. K. *ACS Nano* **2012**, *6*, 2071−2077.
(32) Son, J. G.; Chang, J. -B.; Berggren, K. K.; Ross, C. A. *Nano Lett.* **2011**, *11*, 5079−5084.
(33) Voet, V. S. D.; Pick, T. E.; Park, S. -M.; Moritz, M.; Hammack, A. T.; Urban, J. J.; Ogletree, D. F.; Olynick, D. L.; Helms, B. A. *J. Am. Chem. Soc.* **2011**, *133*, 2812−2815.
(34) Zhang, X.; Murphy, J. N.; Wu, N. L. Y.; Harris, K. D.; Buriak, J. M. *Macromolecules* **2011**, *44*, 9752−9757.
(35) Zhang, X.; Harris, K. D.; Wu, N. L. Y.; Murphy, J. N.; Buriak, J. M. *ACS Nano* **2010**, *4*, 7021−7029.
(36) Kirk, C. T. *Phys. Rev. B* **1998**, *38*, 1255−1273.
(37) Hsieh, I. -F.; Sun, H. -J.; Fu, Q.; Lotz, B.; Cavicchi, K. A.; Cheng, S. Z. D. *Soft Matter* **2012**, *8*, 7937−7944.
(38) Wang, Y.; Hong, X.; Liu, B.; Ma, C.; Zhang, C. *Macromolecules* **2008**, *41*, 5799−5808.
(39) Wang, Z.; Li, B.; Jin, Q.; Ding, D.; Shi, A.-C. *Macromol. Theory Simul.* **2008**, *17*, 301−312.
(40) Wang, Y.; Tong, L.; Steinhart, M. *ACS Nano* **2011**, *5*, 1928−1938.
(41) Tsarkova, L.; Sevink, G. J. A.; Krausch, G. *Adv. Polym. Sci.* **2010**, *227*, 33−73.
(42) Ebnesajjad, S. *Fluoroplastics: Non-Melt Processible Fluoroplastics*; Plastics Digital Library: Norwich, NY, 2000; Vol. *1*, p 27.
(43) Jeong, J. W.; Park, W. I.; Do, L. -M.; Park, J. -H.; Kim, T. -H.; Chae, G.; Jung, Y. S. *Adv. Mater.* **2012**, *24*, 3526.
(44) Kwong, D. -L. *Rapid Thermal and Other Short-Time Processing Technologies II: Proceedings of the International Symposium*; The Electrochemical Society: Pennington, NJ, 2001.
(45) Zohm, H.; Kasper, E.; Mehringer, P.; Muller, G. A. *Microelectron. Eng.* **2000**, *54*, 247−253.
(46) Fitzgerald, T. G.; Farrell, R. A.; Petkov, N.; Bolger, C. T.; Shaw, M. T.; Charpin, J. P. F.; Gleeson, J. P.; Holmes, J. D.; Morris, M. A. *Langmuir* **2009**, *25*, 13551−13560.